

Spectral Analysis of Fake News Propagation

Weibin Cai*

Reza Zafarani*

Abstract. The propagation structure of fake news has been shown to be an important cue for detecting it; yet, existing propagation-based fake news detection methods have mainly relied on ad hoc topological features, and a unified view of cascade patterns is still lacking. To address this, we study news propagation from a spectral view by connecting graph spectra to propagation-related structural properties through rigorous spectral bounds. In particular, we introduce several new bounds and integrate them with existing ones into a unified spectral representation of information propagation. We then use these spectral bounds for downstream classification and design a discrete structural optimization framework to interpret learned propagation patterns. For efficient optimization, we rely on a first-order perturbation approximation and consider both score-guided and bound-guided objectives. Experiments on real-world data reveal meaningful spectral differences between fake and real news, competitive classification performance from spectral bounds, and interpretable evolution trajectories from structural optimization. The findings demonstrate the value of spectral analysis for understanding and modeling news propagation.

1 Introduction. Fake news detection is an important problem because false content can spread rapidly on social media and cause harmful social impact [20, 2, 37]. A natural way to detect fake news is to examine its content or source. Existing early fake news detection methods mainly fall into three categories: *knowledge-based* approaches, which verify claims against external knowledge sources [29, 7]; *style-based* approaches, which exploit linguistic and stylistic cues in news text [44, 46]; and *source-based* approaches, which assess the credibility of the entities involved in news creation, publication, or dissemination [14, 26]. However, these methods all have inherent limitations. Knowledge-based methods depend on reliable external knowledge, which is often incomplete or unavailable in practice [31]. Style-based methods are vulnerable to intentional style manipulation [46], a problem that has become more severe with the rise of generative language models [18]. Source-based methods provide only indi-

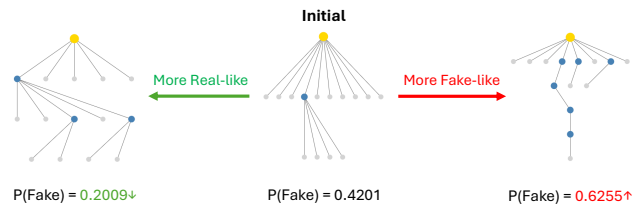


Figure 1.1: The benefits of spectral analysis of news. Illustration of the designed structural optimization from the same initial news propagation tree (nodes are spreaders and edges are spreading patterns). Optimizing (after some steps) toward a more “fake-like” pattern (higher fake probability) produces a **deeper** and more **imbalanced** structure, while optimizing toward a more “real-like” pattern yields a **shallower** and more **balanced** propagation tree.

rect signals, since source credibility does not necessarily imply the veracity of a specific news item. As a result, relying on source credibility alone may lead to overly arbitrary judgments [46]. These methods provide useful signals from the perspectives of *what the news says* and *who is involved in it*, but they do not capture the structural characteristics and diffusion signals of *how the news propagates* on social networks. Prior *propagation-based* studies have shown that fake and real news exhibit different propagation patterns on social networks. For example, fake news tends to spread faster and deeper, and attracts more strongly connected spreaders [37, 45]. These findings suggest that propagation structure provides complementary and robust signals for fake news detection, and has inspired a growing body of structural and graph-based methods [23, 3, 45, 30, 39].

Existing propagation-based methods can be broadly divided into two lines of work. The first line focuses on *neural representation learning* for propagation structures, where graph neural networks [17] and related techniques [40] encode news propagation graphs into latent representations [23, 3, 38, 8]. Although these methods often achieve strong classification performance, the learned representations are difficult to interpret, since individual dimensions usually lack clear structural meaning and the latent space remains hard to analyze directly. The second line uses *handcrafted topological features* to represent propagation graphs [37, 45, 30, 19]. Prior studies have shown that fake news exhibits distinct propagation behaviors from real news through fea-

*Data Lab, Department of EECS, Syracuse University, New York, USA. Emails: weibin44@data.syr.edu, reza@data.syr.edu.

tures such as depth, cascade size, and structural virality [37]. While these handcrafted features provide intuitive insights, they are largely ad hoc and capture only specific aspects of cascade structure rather than offering a unified view of all propagation patterns.

To better understand propagation mechanisms, it is desirable to develop a unified representation of information cascades that can capture global structural patterns, their variations, and help distinguish between different types of cascades (e.g., fake or truth). Spectral graph theory provides a natural path for analyzing propagation graphs. While two cascades may appear similar in size or some topological features, such as depth and structural virality, their underlying “spectral fingerprints,” which are derived from the eigenvalues of matrices such as the adjacency, Laplacian, and normalized Laplacian often reveal fundamental differences in how the information was propagated. These spectra capture global structural properties such as degree distribution, clustering coefficient, connectivity, and the like [15]. Moreover, many cascade characteristics, e.g., breadth, diameter [12], can be linked to eigenvalues through well-established bounds, offering a unified and interpretable representation of propagation structures.

Present work: Spectral Analysis of Fake News.

Motivated by these observations, we study news propagation from a spectral perspective. The key idea is to connect graph spectra with propagation-related structural properties through spectral bounds, and use this connection to analyze how fake and real news differ in their propagation patterns. Under this perspective, we develop two components for propagation analysis. (1) Spectral Representation: We study propagation trees through five general aspects that describe their structure: branching capacity, cascade scale, structural cohesion, propagation span, and diffusion dynamics; each aspect encompasses various cascade properties, which are in turn linked to numerous spectral bounds. Together, these bounds form a unified structural representation of propagation graphs. We further analyze their tightness and correlation with the corresponding graph properties, and test their utility by using them in downstream classification. (2) Structural Optimization: We further develop a discrete structural optimization framework to study how propagation trees evolve under different objectives. This optimization process, using a first-order perturbation approximation, allows us to trace how propagation structures evolve toward a target direction, e.g., fake or real. The result provides insight into the propagation patterns associated with fake and real news. As illustrated in Figure 1.1, the same initial propagation tree can evolve toward more fake-like or more real-like

structures under our optimization framework, revealing clear structural differences between the two. In sum, our contributions are as follows:

- **Spectral analysis of propagation graphs.** We develop a spectral view of news propagation by connecting graph spectra with propagation-related structural properties through spectral bounds. In particular, we prove various new bounds and unify them with existing results to form a propagation-oriented spectral representation. Based on this view, we analyze the differences between fake and real news in their spectra, and study the tightness and correlation of spectral bounds with the corresponding graph properties.
- **Spectral representation of propagation graphs.** We use spectral bounds as a unified structural representation of propagation graphs. To the best of our knowledge, this is the first work to represent news propagation graphs from a spectral perspective. We further validate that these bound-based representations provide informative structural signals for fake news classification.
- **Structural optimization of propagation patterns.** We propose a discrete structural optimization framework to interpret propagation patterns in the space of graphs. Through this optimization, we obtain interpretable structural evolution trajectories and gain deeper insight into the differences between fake and real news propagation.

2 Related Work. As we focus on the propagation structure of fake news, we concentrate on representations that model how news spreads on social networks.

2.1 Neural Representation Learning. Current propagation-based methods can be broadly divided into two types: (1) *homogeneous propagation* models news diffusion using graphs whose nodes are posts and whose edges represent replies or retweets. Representative models such as RvNN [23] and BiGCN [3] build such propagation graphs and use RNNs [5] or GNNs [17] to learn post representations. Some studies further incorporate temporal information, such as posting time, to capture finer-grained diffusion dynamics [35, 28]. Since social media responses may be noisy or intentionally misleading, recent work has also improved robustness through graph contrastive learning [13, 21, 36, 8, 41] and adversarial training [33, 36]. In contrast, (2) *heterogeneous propagation* incorporates richer social context by allowing multiple node and edge types, such as news, posts, and users, together with relations such as posting, replying, retweeting, or following [24, 30]. HPFN [30]

investigates propagation features from structural, temporal, and linguistic perspectives between fake and real news through macro-level (where network includes news nodes, tweet nodes, and retweet nodes) and micro-level (where networks are conversation trees represented by cascade of reply nodes) networks. The authors further incorporate GCNFN [24] into this framework to examine the contribution of different feature types.

2.2 Handcrafted Topological Features. This line of work uses manually designed topological features to characterize propagation cascades. For example, Vosoughi et al. [37] measure static features such as depth, cascade size, maximum breadth, and structural virality [11], together with their temporal evolution, and show that fake news tends to spread deeper, faster, and more broadly than real news. Shu et al. [30] extract the following four topological features in both macro and micro networks: (1) depth; (2) cascade size; (3) maximum outdegree; and (4) depth of the node with the maximum outdegree in macro-level network. They use t -tests to show whether differences between fake news and real news are significant. Zhou et al. [45] categorize propagation-related features into four patterns: (1) more-spreader; (2) farther-distance; (3) stronger-engagement; and (4) dense-networks. Notably, these features are derived from the friendship network of news spreaders rather than the news propagation structure itself. Their analysis shows that fake news tends to spread farther and involve users who are more densely connected and more highly engaged.

3 Preliminaries and Notation. For an undirected graph $G = (V, E)$ with vertices $V = \{v_1, v_2, \dots, v_n\}$ and edges $E \subseteq V \times V$, its adjacency matrix $A \in \mathbb{R}^{n \times n}$ has $A_{ij} = 1$ if $(i, j) \in E$, otherwise 0. The degree matrix $D \in \mathbb{R}^{n \times n}$ is a diagonal matrix with node degrees on its diagonal, i.e., $D_{ii} = \sum_{j=0}^n A_{ij}$. Under news propagation scenario, each node represents a comment or retweet, thus there are no loops in the graph. i.e., propagation graphs are actually trees. Though complex graph structure degrades to trees, many graph properties (e.g. diameter) are still meaningful especially when using spectrum to represent them. The spectrum of a matrix is the set of its eigenvalues, which implicitly reveals its propagation structure properties. A graph can be represented into different matrices defined in terms of A and D , and spectrums of them reflect different characteristics. In this paper, we discuss following three matrices: (1) adjacency matrix A with spectrum $\lambda_1 \geq \lambda_2 \geq \dots \geq \lambda_n$; (2) laplacian matrix $L = D - A$ with spectrum $\mu_1 \geq \mu_2 \geq \dots \geq \mu_n = 0$; (3) normalized laplacian matrix $\mathcal{L} = I - D^{-\frac{1}{2}}AD^{-\frac{1}{2}}$ with spectrum $2 \geq \nu_1 \geq \nu_2 \geq \dots \geq \nu_n = 0$.

4 Spectral Representation of Propagation Graphs. Existing topological features provide intuitive descriptions of propagation trees, but they are often introduced in an ad hoc manner and do not offer a unified view of cascade structure. As a result, they may fail to capture more global aspects of propagation, such as structural robustness and diffusion-related behavior. In contrast, spectral graph theory provides a common language for characterizing graph structure through eigenvalues and eigenvectors. Even when two cascades appear similar under standard topological statistics, their “spectral fingerprints” can still reveal important differences in how information propagates. Motivated by this perspective, we study propagation trees through spectral representation. Directly using the full spectrum, however, is inconvenient because the number of eigenvalues varies with graph size. We therefore organize the spectral representation of news propagation into five complementary categories, each corresponding to one aspect of propagation behavior, such as branching capacity, structural cohesion, and diffusion dynamics. For each category, we use spectral bounds to connect graph spectra with propagation-related structural properties. These bounds include both classical results from spectral graph theory and several new bounds proved in this work. Together, they provide a propagation-oriented and interpretable representation of propagation trees. We next introduce these five categories and their representative spectral bounds to provide an intuitive understanding of the proposed spectral representation.

C1. Branching Capacity reflects how broadly a piece of news can expand at the local level, and prior studies have shown that fake and real news differ noticeably in this aspect [37, 45]. From a spectral perspective, branching capacity is naturally related to the spectral radius λ_1 , which is closely connected to degree concentration through bounds on the maximum and mean degree of a graph. Based on this connection, we further derive λ_1 -based bounds for mean branching, maximum branching at layer k , and degree entropy. The proofs are provided in Appendix A:

PROPOSITION 4.1 (Mean Branching Bound). *Let T be a rooted tree with n nodes and $|I(T)|$ internal nodes. Then, for mean branching \bar{b} ,*

$$\bar{b} \leq \frac{n\lambda_1}{2|I(T)|}.$$

See Appendix A.1 for the proof.

PROPOSITION 4.2 (Maximum Branching at Layer k Bound). *Let T be a rooted tree, and b_k be the number of nodes at level k . Then,*

$$b_k \leq \lambda_1^2(\lambda_1^2 - 1)^{k-1}, \quad k \geq 1.$$

See Appendix A.2 for the proof.

PROPOSITION 4.3 (Degree Entropy Bound). *Let G be a graph with adjacency matrix A , spectral radius λ_1 , and degree distribution $\{q_j\}$, where q_j is the fraction of nodes of degree j . Define the degree entropy by*

$$H_d = - \sum_j q_j \log q_j.$$

Then

$$H_d \leq \log(\lambda_1^2 + 1).$$

See Appendix A.3 for the proof.

C2. Cascade Scale describes the overall size of information diffusion, including how many users and interactions are involved during propagation [37, 30]. In spectral terms, graph size is naturally reflected in the Laplacian spectrum, since $\sum_i \mu_i = \text{trace}(L) = 2(n-1)$. This connection leads to several size-related bounds, such as $\mu_1 \leq n$ and $\mu_2 \leq \lfloor \frac{n}{2} \rfloor$ [42].

C3. Structural Cohesion focuses on how robust and well connected a propagation structure is. Prior studies suggest that fake news is often associated with *echo chambers*, where densely connected clusters are only weakly linked to the rest of the network [45]. A key spectral quantity here is the algebraic connectivity μ_{n-1} . When μ_{n-1} is small, the graph is easier to separate, which indicates weaker cohesion. This motivates the use of quantities such as vertex connectivity [4], which reflects structural robustness, and the Cheeger constant [6], which captures bottlenecks and global constraints in the propagation graph.

C4. Propagation Span characterize how far information propagates and how spread out the cascade becomes. Empirical studies suggest that fake news tends to reach deeper and farther parts of the network [37, 10]. From a spectral perspective, this aspect is closely related to the algebraic connectivity μ_{n-1} . A larger μ_{n-1} usually indicates a more cohesive structure, and therefore shorter distances between nodes; conversely, a smaller μ_{n-1} is often associated with larger propagation span. Based on this connection, we consider spectral bounds for global distance-related quantities, including the diameter [1], and structural virality [32].

C5. Diffusion Dynamics unlike the previous categories, which describe static structural properties of propagation trees, diffusion dynamics concerns how efficiently information flows through the structure. This aspect is naturally linked to the normalized Laplacian spectrum, especially ν_{n-1} , which reflects how quickly diffusion mixes across the graph. Larger values of ν_{n-1} indicate faster mixing and more efficient information spread, while smaller values suggest stronger diffusion

bottlenecks. We therefore use quantities such as random walk convergence and routing time to characterize the dynamic behavior of news propagation [6].

Table C.2 summarizes all bounds, for a total of 35, organized into five categories of propagation structure.

5 Structural Optimization of Propagation Trees. After encoding propagation graphs with spectral bounds and training a classifier, we can further study news propagation patterns through structural optimization. The main idea is to modify an input propagation graph in a controlled direction with the help of the trained classifier. By tracing this structural evolution, we aim to understand how fake and real news differ in their propagation structures.

To this end, we first propose a unified discrete structural optimization algorithm. Within the algorithm, we consider two objectives. (1) **score-guided objective:** we maximize or minimize the predicted probability of being fake for a given graph, so as to observe how the structure changes when the graph becomes more fake-like or more real-like. (2) **Bound-guided objective:** we enforce a specific spectral bound to increase or decrease monotonically, and then examine how the predicted fake probability changes along this process.

5.1 Discrete Structural Optimization. To obtain meaningful evolution paths for propagation graphs, we need to control extraneous variables, such as the number of nodes, while also keeping each modification sufficiently fine-grained. We therefore adopt the following principles:

1. **Scale invariance:** We keep the number of nodes fixed so that the observed changes are purely structural, which avoids size-related bias in the classifier’s prediction.
2. **Structural atomicity:** We define leaf node migration as the minimal unit of structural change. This yields a fine-grained evolution trajectory and supports first-order approximation. Moreover, any size-preserving structural change can be viewed as a sequence of leaf node migrations.

Based on these two principles, we present the abstract pipeline of our discrete structural optimization in Algorithm 5.1, where different objective functions can be specified in line 1. We then consider two objectives: (1) optimizing the current fake news prediction score in Section 5.2; and (2) optimizing a specific propagation structure in Section 5.3.

5.2 Score-guided Optimization. We aim to decode the knowledge learned by the classifier into discrete graph topology. More specifically, given a fixed

Algorithm 5.1 Discrete Structural Optimization

Input: Initial tree G_0 , Iterations T
Output: Evolved tree sequence $\mathcal{H} = \{G_0, G_1, \dots, G_k\}$
1: Define objective function: $\Phi(G)$
2: Initialize: $\mathcal{H} := \{G_0\}$
3: **for** $t = 0$ **to** T **do**
4: $\mathcal{N}(G_t) := \{\text{all possible leaf migrations on } G_t\}$
5: $\delta^* := \operatorname{argmax}_{\delta \in \mathcal{N}(G_t)} \Phi(G_t \oplus \delta)$
6: $G_{t+1} := G_t \oplus \delta^*$
7: $\mathcal{H} := \mathcal{H} \cup \{G_{t+1}\}$
8: **end for**
9: **return** \mathcal{H}

number of nodes, we ask what kind of propagation structure the classifier considers more characteristic of fake news. The full pseudo code is shown in Algorithm 5.2. In line 1, we use the prediction score as the objective function. We use d to control the direction of evolution, where $d = 1$ ($d = -1$) drives the graph toward a more fake-like (real-like) structure. During the evolution process (lines 4–20), we first enumerate all possible leaf node migrations \mathcal{P} (lines 5–13). Each candidate migration consists of a leaf node v , its current parent p_{old} , and a new parent p_{new} . For each candidate, we input the resulting graph into the classifier, compute the prediction score, and select the migration that gives the best objective value as the action at step t (lines 8–12). After each action, we check whether the objective value S has converged using a threshold τ (lines 14–19). After optimization, we obtain an evolved tree sequence \mathcal{H} that reveals intuitive structural patterns associated with fake or real news propagation, and also provides an interpretable view of the classifier’s behavior.

5.3 Bound-guided Optimization. In Section 5.2, we optimize propagation structures indirectly through the classifier score, and then infer the global propagation patterns of fake and real news. In this section, we instead optimize specific structural bounds directly and examine how the evolution of these structural properties affects the fake news prediction. The full pseudo code is presented in Algorithm 5.3.

To optimize a target bound through leaf-node migration, we must evaluate how each candidate migration changes that bound. A direct approach is to compute the eigenvalues of every resulting graph exactly, and then use them to calculate the target bound. However, the number of candidate migrations in one step is usually large, ranging from $n - 1$ to $(n - 1)^2$, where n is the number of nodes. For a path graph, there are $n - 1$ possible migrations, while for a star graph, there are $(n - 1)^2$. As a result, performing eigendecomposition for all candidates at every step is computationally expensive. To balance computational cost and estimation of accuracy, we propose a first-order approximation method to es-

Algorithm 5.2 Score-guided Optimization

Input: Initial tree G_{init} , Model \mathcal{M} , Iterations T , Direction $d \in \{1, -1\}$, Convergence threshold τ
Output: Evolved sequence $\mathcal{H} = \{(G_0, S_0), \dots, (G_k, S_k)\}$
1: Define objective: $\Phi(G) = d \cdot \operatorname{Prob}_{\mathcal{M}}(\text{fake} \mid G)$
2: $G_{\text{cur}} \leftarrow G_{\text{init}}$
3: $\mathcal{H} \leftarrow \{(G_{\text{cur}}, \Phi(G_{\text{cur}}))\}$
4: **for** $t = 1$ **to** T **do**
5: $\mathcal{N}(G_{\text{cur}}) \leftarrow \{\text{all valid leaf-node migrations } \delta = (v, p_{\text{old}}, p_{\text{new}})\}$
6: $G^*, S^* \leftarrow \text{None}, \text{None}$
7: **for all** candidate move $\delta \in \mathcal{N}(G_{\text{cur}})$ **do**
8: $G' \leftarrow G_{\text{cur}} \oplus \delta$
9: $S' \leftarrow \Phi(G')$
10: **if** $S' > S^*$ **then**
11: $G^*, S^* \leftarrow G', S'$
12: **end if**
13: **end for**
14: **if** $(S^* - S_{\text{cur}}) > \tau$ **then**
15: $G_{\text{cur}}, S_{\text{cur}} \leftarrow G^*, S^*$
16: $\mathcal{H} \leftarrow \mathcal{H} \cup \{(G_{\text{cur}}, S_{\text{cur}})\}$
17: **else**
18: **break**
19: **end if**
20: **end for**
21: **return** \mathcal{H}

timate the eigenvalue change caused by each leaf-node migration, as stated in Proposition 5.1.

PROPOSITION 5.1. *Let T be a tree and u_i be its i -th orthonormal Laplacian eigenvector. When we move a leaf node v from p_{old} to p_{new} , we can estimate the change of each eigenvalue μ_i by*

$$(5.1) \quad \Delta\mu_i \approx (u_i[v] - u_i[p_{\text{new}}])^2 - (u_i[v] - u_i[p_{\text{old}}])^2,$$

Proof. Let $Lu = \mu u$. After a small perturbation ΔL , we have

$$(5.2) \quad (L + \Delta L)(u + \Delta u) = (\mu + \Delta\mu)(u + \Delta u).$$

Ignoring higher-order terms, we obtain

$$(5.3) \quad L\Delta u + \Delta Lu \approx \mu\Delta u + \Delta\mu u.$$

Left-multiplying by u^T yields

$$(5.4) \quad u^T L\Delta u + u^T \Delta Lu \approx \mu u^T \Delta u + \Delta\mu u^T u.$$

As L is symmetric, $u^T L = \mu u^T$, and $u^T u = 1$, so

$$(5.5) \quad \Delta\mu \approx u^T \Delta Lu.$$

For adding new edge (r, c) , the perturbation matrix can be written as

$$(5.6) \quad \Delta L = (e_r - e_c)(e_r - e_c)^T,$$

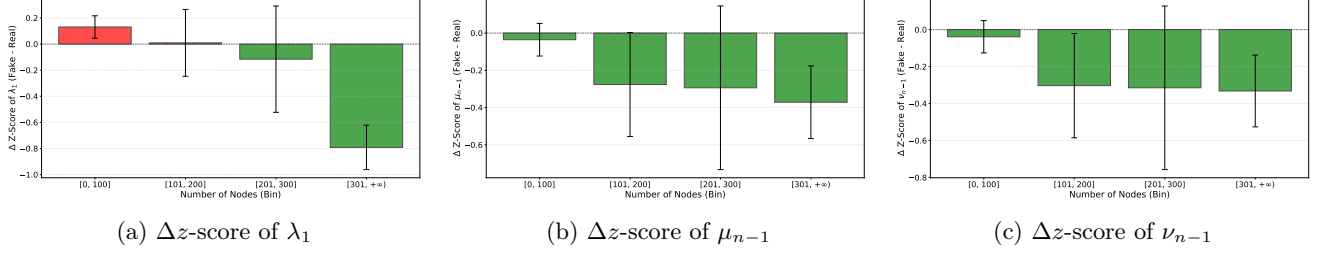


Figure 5.1: Mean z -score differences across node-count bins for three eigenvalues, λ_1 , μ_{n-1} , and ν_{n-1} , on the Weibo22 dataset. Red indicates that eigenvalues of fake news are larger than real news, while green indicates the opposite.

Algorithm 5.3 Bound-guided Optimization

Input: Initial tree G_0 , Max iterations T , Direction $d \in \{1, -1\}$, Convergence threshold τ

Output: Evolution sequence $\mathcal{H} = \{G_0, G_1, \dots, G_k\}$

- 1: Define objective: $\Phi(G) = d \cdot \mathcal{B}(\mu_1, \dots, \mu_n)$
 - 2: $G_{cur} \leftarrow G_0$, $\mathcal{H} \leftarrow \{G_0\}$
 - 3: **for** $t = 0$ **to** T **do**
 - 4: Compute all eigenvalues $\{\mu_i\}$ and eigenvectors $\{\mathbf{u}_i\}$ for G_{cur}
 - 5: $\mathcal{N}(G_{cur}) \leftarrow \{\text{all valid leaf-node migrations } \delta = (v, p_{old}, p_{new})\}$
 - 6: **for all** candidate move $\delta \in \mathcal{N}(G_{cur})$ **do**
 - 7: $\Delta\mu_i(\delta) \approx (u_i[v] - u_i[p_{new}])^2 - (u_i[v] - u_i[p_{old}])^2$, $\forall i$
 - 8: $\tilde{\mu}_i \leftarrow \mu_i + \Delta\mu_i(\delta)$
 - 9: $\tilde{\Phi}(\delta) \leftarrow d \cdot \mathcal{B}(\tilde{\mu}_1, \dots, \tilde{\mu}_n)$
 - 10: **end for**
 - 11: $\delta^* = \arg \max_{\delta \in \mathcal{N}(G_{cur})} [\tilde{\Phi}(\delta)]$
 - 12: **if** $\tilde{\Phi}(\delta^*) - \Phi(G_{cur}) > \tau$ **then**
 - 13: $G_{cur} \leftarrow G_{cur} \oplus \delta^*$
 - 14: $\mathcal{H} \leftarrow \mathcal{H} \cup \{G_{cur}\}$
 - 15: **else**
 - 16: **break**
 - 17: **end if**
 - 18: **end for**
 - 19: **return** \mathcal{H}
-

where e_r is the standard basis vector.

Substituting Eq. 5.6 into Eq. 5.5, we obtain

$$(5.7) \quad \Delta\mu_{\text{add}(r,c)} \approx (u_r - u_c)^2.$$

Similarly, for deleting an edge (r, c) , we have

$$(5.8) \quad \Delta\mu_{\text{delete}(r,c)} \approx -(u_r - u_c)^2. \quad \square$$

By adding Eq 5.7 and Eq 5.8, we can get Eq 5.1.

The same derivation can be applied to other types of eigenvalues, such as λ_i and ν_i . In particular, we obtain

$$(5.9) \quad \Delta\lambda_i \approx 2u_i[v](u_i[p_{\text{new}}] - u_i[p_{\text{old}}]).$$

As the perturbation induced by a leaf-node migration is small, this first-order approximation works well in practice. The accuracy also tends to improve as the graph grows. For further analysis see Appendix B.

Time Complexity. Let n be the number of nodes in the current propagation graph, and M be the number of valid leaf-node migrations in one iteration. As M ranges from $O(n)$ to $O(n^2)$, corresponding to chain and star graphs in the extreme cases, the cost of exact bound-guided optimization can be high. Without approximation, we need to recompute the eigendecomposition for every candidate migration, which gives a per-iteration time complexity of $O(Mn^3)$. This ranges from $O(n^4)$ to $O(n^5)$. With first-order approximation, we perform eigendecomposition only once for the current graph, costing $O(n^3)$, and then evaluate each candidate migration in $O(n)$ time by estimating the change of eigenvalues. The resulting per-iteration complexity is $O(n^3 + Mn)$, dominated by $O(n^3)$. So, the approximation reduces per-iteration cost from $O(Mn^3)$ to $O(n^3)$.

6 Experiments. We conduct a series of experiments to evaluate the proposed framework. First, we perform exploratory analyses of eigenvalues and spectral bounds in the news propagation setting. This allows us to examine whether fake and real news exhibit distinct structural differences, and to assess the tightness of the bounds introduced in Section 4. Second, we use these bounds as graph encodings for the downstream fake news classification task, in order to evaluate their effectiveness. Finally, based on the trained classifier, we apply the discrete structural optimization algorithm proposed in Section 5. This helps us obtain an intuitive understanding of the differences between fake and real news propagation patterns. More details about datasets and settings are provided in Appendix C.

6.1 Analysis of Eigenvalue Distribution. We compute the eigenvalues of every propagation graph in the Weibo22 dataset. For fake and real news separately, we then standardize each eigenvalue by its z -score and compute the mean Δz -score, defined as the fake-news mean minus the real-news mean, for each eigenvalue. Figure 5.1 shows the distributions of λ_1 , μ_{n-1} , and ν_{n-1} .

(1) Figure 5.1a shows that, for small propagation graphs, fake news usually has a larger λ_1 . This suggests the presence of more highly connected hub nodes and

Table 6.1: Comparison of spectral bounds for estimating structural properties on the Weibo22 dataset. Entries marked with * are statistically significant at $p < 0.05$. The bound formulas in the upper part of the table directly correspond to the meanings of the associated structural features, whereas those in the lower part do not. In the lower part, we further examine the relationship between the structure virality bound and the actual diameter, as well as the relationship between the max-breadth bound and the actual number of leaf nodes.

Bound Equation	Structural Feature	Rel. Error (ϵ)	Spearman (ρ)	Kendall (τ)	Pearson (r)
λ_1	max degree	0.69 ± 0.23	0.999*	0.987*	0.905*
$\# \text{ distinct } \mu_i - 1$	diameter	5.29 ± 8.1	0.867*	0.718*	0.677*
μ_1	num nodes	0.18 ± 0.20	0.989*	0.928*	0.934*
$\lambda_1^2(\lambda_1^2 - 1)^0$ (k=1)	max-breadth	0.08 ± 0.21	0.998*	0.981*	0.998*
$\frac{2}{n-1} \sum 1/\mu_i$	diameter	0.43 ± 0.20	0.930*	0.799*	0.899*
$\lambda_1^2(\lambda_1^2 - 1)^0$ (k=1)	# leaf node	0.14 ± 0.22	0.996*	0.959*	0.955*

a stronger ability for global diffusion. However, as the graph size increases, the λ_1 of real news becomes larger than that of fake news. This indicates that we *cannot simply conclude that fake news spreads more broadly without considering graph size and related factors*.

(2) Figure 5.1b shows that real news usually has a larger μ_{n-1} , which indicates a smaller graph diameter. A smaller diameter often corresponds to a shallower propagation depth. This is consistent with the finding that *fake news tends to spread deeper* [37, 45].

(3) Figure 5.1c shows that fake news often has a smaller ν_{n-1} . This suggests a smaller *Cheeger constant*, meaning that *fake news propagation graphs tend to be less well connected, show clearer community separation, and are more prone to fragmentation*.

Overall, these observations suggest that eigenvalues can help distinguish fake news from real news. They also provide a certain degree of structural interpretability.

6.2 Analysis of Bounds Tightness. We further examine whether the spectral bounds introduced in Section 4 can faithfully reflect true graph properties in the news propagation setting. We evaluate the quality of these bounds from two perspectives: (1) **Tightness**, measuring how close a bound is to the corresponding graph property. We use the relative error $\epsilon_i = \frac{|q_i - b_i|}{q_i}$, where q_i denotes the true quantity and b_i denotes its corresponding bound. A smaller ϵ_i shows a tighter bound. We compute the relative error for each graph in our data and report the mean value. (2) **Consistency**, measuring whether a bound preserves the relationship with the true property even when the numerical gap is large. We evaluate consistency from three aspects: (i) linear correlation, measured by Pearson’s r [27]; (ii) monotonic correlation, measured by Spearman’s ρ [34]; and (iii) pairwise agreement, measured by Kendall’s τ [16]. The results are in Table 6.1.

The results show two main findings. First, many spectral bounds are useful proxies for their corresponding graph properties. Some are reasonably tight

with relative errors below 0.70, while others remain highly correlated with the true quantities even when the numerical gap is larger. This indicates that spectral bounds can still provide reliable structural signals for characterizing news propagation. Second, cross-property comparisons reveal structural characteristics of dataset itself. For example, the structure virality bound is even closer to the true diameter than the diameter bound itself, and the max-breadth bound is close to the number of leaf nodes. Together, these observations suggest that propagation in Weibo22 tends to be relatively star-like.

Table 6.2: Comparing classification performance on Weibo22 and Twitter16. The best and second-best results are in bold and italics, respectively. Ties are broken by smaller standard deviation. Categories are abbreviated.

Method	Weibo22		Twitter16	
	ACC	F1	ACC	F1
Random	47.92	49.16	22.98	22.94
Structural Features	59.65	56.52	33.03	30.79
GCN	48.86	47.77	27.42	27.35
Bound Features	59.40	<i>57.65</i>	33.55	32.20
- <i>C1. Branching</i>	<i>59.47</i>	57.96	33.16	31.51
- <i>C2. Scale</i>	59.29	57.70	33.16	31.11
- <i>C3. Cohesion</i>	59.25	57.70	33.55	<i>31.83</i>
- <i>C4. Span</i>	57.88	55.64	33.55	31.69
- <i>C5. Diffusion</i>	58.31	54.53	<i>33.55</i>	31.77

6.3 Effectiveness of Bounds in Classification. To evaluate the effectiveness of spectral bounds in the downstream fake news classification using only structural information, we compare bound-based features with other structure-only methods, including hand-crafted topological features and GCN [17]. More details about the baselines are provided in Appendix C.2. The results in Table 6.2 show that both bound-based features and topological features perform much better than GCN. Moreover, bound-based features achieve performance comparable to topological features, even though some bounds are not numerically

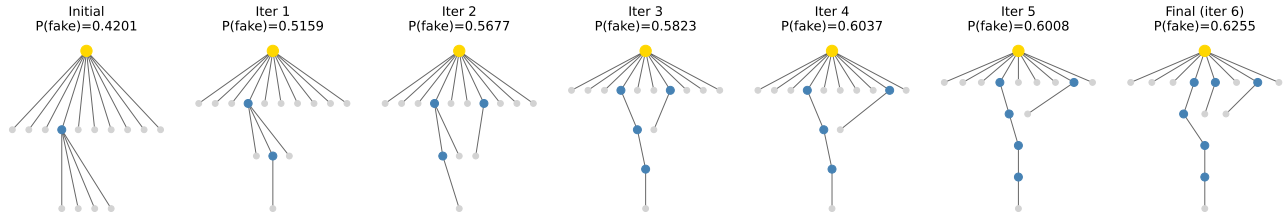


Figure 6.1: Propagation graph evolution toward a more fake news like structure under score-guided optimization. Yellow, blue, and gray nodes denote the root, internal, and leaf nodes, respectively. The title of each graph shows the current iteration t and the classifier prediction score.

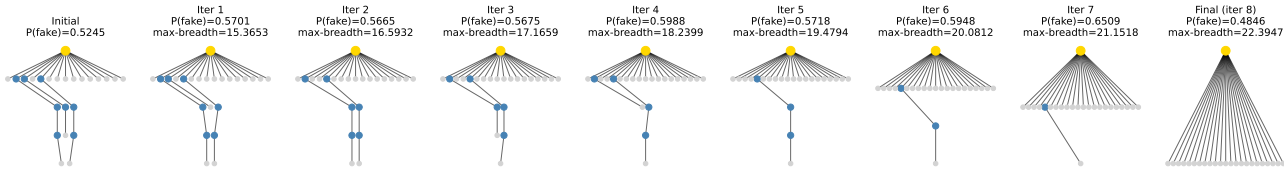


Figure 6.2: Propagation graph evolution toward higher max-breadth under bounds-guided optimization. Yellow, blue, and gray nodes denote the root, internal, and leaf nodes, respectively. The title of each graph shows the current iteration t , the classifier prediction score, and bound value.

close to their exact properties. This suggests that spectral bounds still capture highly informative structural signals for distinguishing fake news from real news. In addition, by ablating the bounds in each category, we find that different datasets show different preferences over structural aspects. For example, on *Weibo22*, fake and real news differ more clearly in *C4. Propagation Span* and *C5. Diffusion Dynamics*, which is consistent with the distributional patterns in Figure 5.1. In contrast, on *Twitter16*, the differences are more pronounced in *C1. Branching Capacity* and *C2. Cascade Scale*. This suggests that the propagation patterns of fake and real news may vary across events or platforms.

6.4 Evolution of Propagation Structures.

We apply algorithms proposed in Section 5 with the trained classifier from Section 6.3 to obtain Figure 6.1 and Figure 6.2. The figures provide a deeper understanding about fake news propagation patterns. More cases can be found in Appendix D.

Evolution Toward “More Fake.” *Although fake news propagation is often deeper and more unbalanced, increasing these factors alone does not always make a cascade more fake-like.* Figure 6.1 shows that the graph evolves from an initial depth of 2 to a final depth of 5, while becoming more unbalanced as a deep subtree gradually emerges. This suggests that fake-like propagation tends to be associated with deeper and more unbalanced structures. However, the effect is not monotonic. From iter 4 to iter 5, the depth increases but $P(\text{fake})$ decreases. From iter 5 to iter 6, the algorithm does not further increase depth, but instead moves a

first-layer node to the second layer, which raises $P(\text{fake})$.

Evolution Toward Higher Max-Breadth. *Although prior studies suggest that fake news typically spreads more broadly [37], a broader propagation pattern does not necessarily make a cascade more fake-like.* Figure 6.2 shows that as the graph evolves to increase max-breadth, $P(\text{fake})$ does not follow a stable monotonic trend. For example, the trees at iter 4 and iter 5 have the same depth, but the broader tree at iter 5 still receives a lower $P(\text{fake})$. From iter 5 to iter 8, depth continues to decrease and breadth continues to increase, yet $P(\text{fake})$ keeps rising. However, in the final iteration, $P(\text{fake})$ drops sharply. This suggests that whether a propagation pattern appears more fake-like or more real-like depends on the overall structural configuration, rather than on any single factor alone.

Together, these evolutions suggest that *fake-like propagation depends on a more specific structural configuration than simply being deeper, unbalanced, or broader.*

7 Conclusion. This paper studies fake news propagation from a spectral perspective. Our results show that graph spectra and spectral bounds provide a useful way to characterize propagation structure beyond independently designed topological features. Through this perspective, we find that fake and real news exhibit meaningful differences in their spectral patterns, and that many propagation-related properties can be effectively analyzed through spectral bounds. Beyond representation, our decoding results further suggest that the proposed spectral view is also useful for interpretation. By tracing how propagation trees evolve under different

objectives, we obtain intuitive structural patterns associated with fake and real news. Overall, this work shows that spectral analysis offers a unified and interpretable direction for understanding news propagation.

References

- [1] N. ALON AND V. D. MILMAN, λ_1 , isoperimetric inequalities for graphs, and superconcentrators, *Journal of Combinatorial Theory, Series B*, 38 (1985), pp. 73–88.
- [2] J. BAKDASH, C. SAMPLE, M. RANKIN, M. KANTARCIOGLU, J. HOLMES, S. KASE, E. ZAROUKIAN, AND B. SZYMANSKI, *The future of deception: Machine-generated and manipulated images, video, and audio?*, in 2018 International Workshop on Social Sensing (SocialSens), IEEE, 2018, pp. 2–2.
- [3] T. BIAN, X. XIAO, T. XU, P. ZHAO, W. HUANG, Y. RONG, AND J. HUANG, *Rumor detection on social media with bi-directional graph convolutional networks*, in Proceedings of the AAAI conference on artificial intelligence, vol. 34, 2020, pp. 549–556.
- [4] A. E. BROUWER AND W. H. HAEMERS, *Spectra of graphs*, Springer Science & Business Media, 2011.
- [5] K. CHO, B. VAN MERRIËNBOER, D. BAHDANAU, AND Y. BENGIO, *On the properties of neural machine translation: Encoder-decoder approaches*, arXiv preprint arXiv:1409.1259, (2014).
- [6] F. R. CHUNG, *Spectral graph theory*, vol. 92, American Mathematical Soc., 1997.
- [7] G. L. CIAMPAGLIA, P. SHIRALKAR, L. M. ROCHA, J. BOLLEN, F. MENCZER, AND A. FLAMMINI, *Computational fact checking from knowledge networks*, *PloS one*, 10 (2015), p. e0128193.
- [8] C. CUI AND C. JIA, *Propagation tree is not deep: Adaptive graph contrastive learning approach for rumor detection*, in Proceedings of the AAAI Conference on artificial intelligence, vol. 38, 2024, pp. 73–81.
- [9] K. C. DAS AND P. KUMAR, *Some new bounds on the spectral radius of graphs*, *Discrete Mathematics*, 281 (2004), pp. 149–161.
- [10] A. FRIGGERI, L. ADAMIC, D. ECKLES, AND J. CHENG, *Rumor cascades*, in proceedings of the international AAAI conference on web and social media, vol. 8, 2014, pp. 101–110.
- [11] S. GOEL, A. ANDERSON, J. HOFMAN, AND D. J. WATTS, *The structural virality of online diffusion*, *Management science*, 62 (2016), pp. 180–196.
- [12] J. GUO, J. XUE, AND R. LIU, *Laplacian eigenvalue distribution, diameter and domination number of trees*, *Linear and Multilinear Algebra*, 73 (2025), pp. 763–775.
- [13] Z. HE, C. LI, F. ZHOU, AND Y. YANG, *Rumor detection on social media with event augmentations*, in Proceedings of the 44th international ACM SIGIR conference on research and development in information retrieval, 2021, pp. 2020–2024.
- [14] B. D. HORNE, W. DRON, S. KHEDR, AND S. ADALI, *Assessing the news landscape: A multi-module toolkit for evaluating the credibility of news*, in Companion Proceedings of the The Web Conference 2018, 2018, pp. 235–238.
- [15] S. JIN AND R. ZAFARANI, *The spectral zoo of networks: Embedding and visualizing networks with spectral moments*, in Proceedings of the 26th ACM SIGKDD International Conference on Knowledge Discovery & Data Mining, 2020, pp. 1426–1434.
- [16] M. G. KENDALL, *A new measure of rank correlation*, *Biometrika*, 30 (1938), pp. 81–93.
- [17] T. KIPF, *Semi-supervised classification with graph convolutional networks*, arXiv preprint arXiv:1609.02907, (2016).
- [18] S. KUMAR, S. SAI, V. CHAMOLA, A. GAUR, C. AGARWAL, K. HUANG, AND A. HUSSAIN, *Peeping into the future: Understanding and combating generative ai-based fake news*, *Cognitive Computation*, 17 (2025), p. 103.
- [19] S. KWON, M. CHA, K. JUNG, W. CHEN, AND Y. WANG, *Prominent features of rumor propagation in online social media*, in 2013 IEEE 13th international conference on data mining, IEEE, 2013, pp. 1103–1108.
- [20] D. M. LAZER, M. A. BAUM, Y. BENKLER, A. J. BERINSKY, K. M. GREENHILL, F. MENCZER, M. J. METZGER, B. NYHAN, G. PENNYCOOK, D. ROTHSCHILD, ET AL., *The science of fake news*, *Science*, 359 (2018), pp. 1094–1096.
- [21] G. MA, C. HU, L. GE, J. CHEN, H. ZHANG, AND R. ZHANG, *Towards robust false information detection on social networks with contrastive learning*, in Proceedings of the 31st ACM international conference on information & knowledge management, 2022, pp. 1441–1450.

- [22] J. MA, W. GAO, AND K.-F. WONG, *Detect rumors in microblog posts using propagation structure via kernel learning*, in Proceedings of the 55th Annual Meeting of the Association for Computational Linguistics (Volume 1: Long Papers), 2017, pp. 708–717.
- [23] J. MA, W. GAO, AND K.-F. WONG, *Rumor detection on twitter with tree-structured recursive neural networks*, Association for Computational Linguistics, 2018.
- [24] F. MONTI, F. FRASCA, D. EYNARD, D. MANIÖN, AND M. M. BRONSTEIN, *Fake news detection on social media using geometric deep learning*, ArXiv, abs/1902.06673 (2019), <https://api.semanticscholar.org/CorpusID:62841478>.
- [25] K. NADERI AND K. PANKRASHKIN, *Introduction to Spectral Graph Theory*, Springer Nature, 2026.
- [26] J. NÖRREGAARD, B. D. HORNE, AND S. ADALI, *Nela-gt-2018: A large multi-labelled news dataset for the study of misinformation in news articles*, in Proceedings of the international AAAI conference on web and social media, vol. 13, 2019, pp. 630–638.
- [27] K. PEARSON, *Vii. note on regression and inheritance in the case of two parents*, proceedings of the royal society of London, 58 (1895), pp. 240–242.
- [28] X. PENG, J. WU, R. LIU, AND K. XU, *Rumor detection on social media with temporal propagation structure optimization*, arXiv preprint arXiv:2412.08316, (2024).
- [29] B. SHI AND T. WENINGER, *Discriminative predicate path mining for fact checking in knowledge graphs*, Knowledge-based systems, 104 (2016), pp. 123–133.
- [30] K. SHU, D. MAHUESWARAN, S. WANG, AND H. LIU, *Hierarchical propagation networks for fake news detection: Investigation and exploitation*, in Proceedings of the international AAAI conference on web and social media, vol. 14, 2020, pp. 626–637.
- [31] K. SHU, A. SLIVA, S. WANG, J. TANG, AND H. LIU, *Fake news detection on social media: A data mining perspective*, ACM SIGKDD explorations newsletter, 19 (2017), pp. 22–36.
- [32] S. SIVASUBRAMANIAN, *Average distance in graphs and eigenvalues*, Discrete mathematics, 309 (2009), pp. 3458–3462.
- [33] Y.-Z. SONG, Y.-S. CHEN, Y.-T. CHANG, S.-Y. WENG, AND H.-H. SHUAI, *Adversary-aware rumor detection*, in Findings of the Association for Computational Linguistics: ACL-IJCNLP 2021, 2021, pp. 1371–1382.
- [34] C. SPEARMAN, *The proof and measurement of association between two things.*, (1961).
- [35] M. SUN, X. ZHANG, J. ZHENG, AND G. MA, *Ddgc: Dual dynamic graph convolutional networks for rumor detection on social media*, in Proceedings of the AAAI conference on artificial intelligence, vol. 36, 2022, pp. 4611–4619.
- [36] T. SUN, Z. QIAN, S. DONG, P. LI, AND Q. ZHU, *Rumor detection on social media with graph adversarial contrastive learning*, in Proceedings of the ACM web conference 2022, 2022, pp. 2789–2797.
- [37] S. VOSOUGHI, D. ROY, AND S. ARAL, *The spread of true and false news online*, science, 359 (2018), pp. 1146–1151.
- [38] L. WEI, D. HU, W. ZHOU, AND S. HU, *Uncertainty-aware propagation structure reconstruction for fake news detection*, in Proceedings of the 29th international conference on computational linguistics, 2022, pp. 2759–2768.
- [39] K. WU, S. YANG, AND K. Q. ZHU, *False rumors detection on sina weibo by propagation structures*, in 2015 IEEE 31st international conference on data engineering, IEEE, 2015, pp. 651–662.
- [40] Y. YOU, T. CHEN, Y. SUI, T. CHEN, Z. WANG, AND Y. SHEN, *Graph contrastive learning with augmentations*, Advances in neural information processing systems, 33 (2020), pp. 5812–5823.
- [41] J. ZHANG, Z. LI, Q. LIU, S. WU, Z. WANG, AND L. WANG, *Evolving to the future: Unseen event adaptive fake news detection on social media*, in Proceedings of the 33rd ACM International Conference on Information and Knowledge Management, 2024, pp. 4273–4277.
- [42] X.-D. ZHANG, *The laplacian eigenvalues of graphs: a survey*, arXiv preprint arXiv:1111.2897, (2011).
- [43] Y. ZHANG, K. XIE, X. ZHANG, X. DONG, AND S. WANG, *Rumor detection on social media with reinforcement learning-based key propagation graph generator*, in Proceedings of the ACM on Web Conference 2025, 2025, pp. 2742–2753.

- [44] X. ZHOU, A. JAIN, V. V. PHOHA, AND R. ZAFARANI, *Fake news early detection: An interdisciplinary study*, arXiv preprint arXiv:1904.11679, (2019).
- [45] X. ZHOU AND R. ZAFARANI, *Network-based fake news detection: A pattern-driven approach*, ACM SIGKDD explorations newsletter, 21 (2019), pp. 48–60.
- [46] X. ZHOU AND R. ZAFARANI, *A survey of fake news: Fundamental theories, detection methods, and opportunities*, ACM Computing Surveys (CSUR), 53 (2020), pp. 1–40.

A Spectral Bounds Details. We list all bounds in Table C.2. Here are our proofs for mean branching, maximum branching at layer k , and degree entropy:

LEMMA A.1. [9] *Let T be a tree with n nodes, Let Δ be the maximum degree of T , then we have*

$$(A.1) \quad \Delta \leq \lambda_1^2$$

A.1 Proof of Proposition 4.1 (Mean Branching Bound)

Proof. Let k_v be the number of children of an internal node v . Then

$$\bar{b} = \frac{1}{|I(T)|} \sum_{v \in V_{\text{int}}} k_v.$$

Since every edge in a rooted tree contributes exactly once to a parent-child relation,

$$\sum_{v \in V_{\text{int}}} k_v = n - 1.$$

Thus

$$\bar{b} = \frac{n - 1}{|I(T)|}.$$

On the other hand, the average degree is

$$\bar{d} = \frac{2(n - 1)}{n}.$$

Hence

$$\bar{b} = \frac{n}{2|I(T)|} \bar{d}.$$

Using the standard bound $\bar{d} \leq \lambda_1$ [4], we obtain

$$\bar{b} \leq \frac{n\lambda_1}{2|I(T)|}.$$

A.2 Proof of Proposition 4.2 (Maximum Branching at Layer k)

Proof. Let Δ be the maximum degree of T . The root has at most Δ children, so

$$b_1 \leq \Delta.$$

For $k \geq 2$, each node at level $k - 1$ has at most $\Delta - 1$ children, since one incident edge is used by its parent. Therefore,

$$b_k \leq \Delta(\Delta - 1)^{k-1}.$$

Now we leverage Lemma A.1 by substituting, which yields

$$b_k \leq \lambda_1^2(\lambda_1^2 - 1)^{k-1}. \quad \square$$

A.3 Proof of Proposition 4.3 (Degree Entropy Bound)

Proof. Let K denote the number of distinct degree values that appear in G . Since degrees are integers between 0 and the maximum degree Δ , we have

$$K \leq \Delta + 1.$$

For a discrete distribution supported on K values, entropy is maximized by the uniform distribution. Hence

$$H_d = - \sum_j q_j \log q_j \leq \log K \leq \log(\Delta + 1).$$

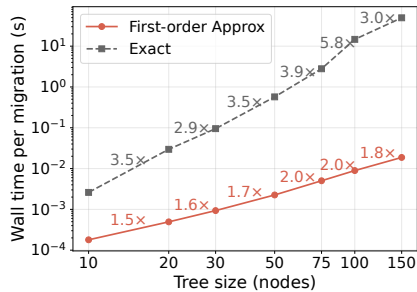
Since we already know $\Delta \leq \lambda_1^2$ from Lemma A.1, thus

$$H_d \leq \log(\Delta + 1) \leq \log(\lambda_1^2 + 1). \quad \square$$

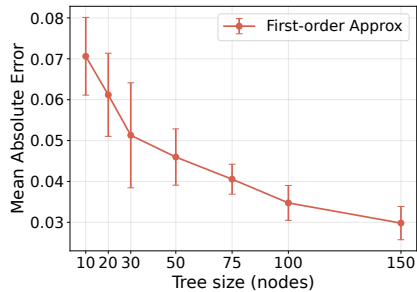
B Computational Analysis of First-Order Approximation.

To evaluate the efficiency and accuracy of the proposed first-order approximation, we compare it with the exact method, which recomputes eigenvalues by eigendecomposition on the Weibo22 dataset. Specifically, we consider a range of target tree sizes, [10, 20, 30, 50, 75, 100, 150], and for each size randomly sample up to 20 trees whose node counts differ by at most 3 from the target. We then apply both methods to these trees to compute our target eigenvalue after per migration and compare them in terms of: (1) practical running time, measured by wall time per migration; and (2) approximation quality, measured by the mean absolute error (MAE) and Spearman's ρ . We report the mean and standard deviation over all sampled trees. We use λ_1 , which is involved in the max-breadth bound 4.2, as the target quantity. The results are shown in Figure A.1.

\square **Efficiency.** Figure A.1a shows that the first-order approximation is consistently faster than the exact



(a) Wall time across tree size.



(b) MAE across tree size.

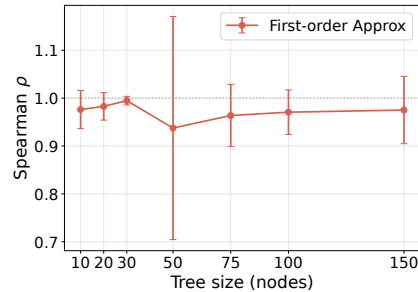
(c) Spearman ρ across tree size.

Figure A.1: Efficiency and accuracy of the first-order approximation on the Weibo22 dataset, using λ_1 as the target quantity. In Figure A.1a, both axes are shown on a log scale, and the numbers annotated along the curves indicate the corresponding slopes in the log-log plot.

method. On the log-log scale, the approximation grows much more slowly with tree size. For small trees with 10 nodes, it is already about one order of magnitude faster. When the tree size reaches 150, the gap increases to roughly three orders of magnitude. This confirms that the approximation substantially reduces the computational cost of bound-guided optimization in practice.

Accuracy. Figures A.1b and A.1c show that the approximation remains accurate across all tree sizes. As the number of nodes increases, the MAE steadily decreases, while the average Spearman’s ρ stays above 0.9. Notably, larger trees also induce substantially more candidate leaf-node migrations, typically growing toward $O(n^2)$, which makes candidate ranking increasingly difficult. Even under this harder setting, the first-order approximation still preserves the ranking of candidate migrations well. This indicates that it remains reliable for guiding bound-guided optimization, especially on larger graphs.

C Experiments Details. We provide details about settings of experiments, which include datasets, and baselines.

C.1 Dataset Details. We use Weibo22 [43] and Twitter16 [22]. We only use the graph with more than 3 nodes and less than 10,000 nodes. Statistics can be seen from Table C.1.

C.2 Classification Experiment Details. We apply 5-fold cross-validation on every model. Their respective settings are as follows:

- **Random:** we uniformly sample labels from $(0, 1)$ as prediction;
- **GCN:** we use random features as node features since we only use structure information. We further manually tune hyperparameters and select the best

Table C.1: Statistics of Twitter16 and Weibo22.

Statistic	Twitter16	Weibo22
# Graphs	766	2761
# Non-rumors	205	1247
# False rumors	180	1514
# True rumors	196	0
# Unverified rumors	185	0
Avg # Nodes	24.2	228.3
Med # Nodes	14	20
Max # Nodes	250	9495

as final parameters. Finally, we set number of layers as 2, hidden dimension as 64, node feature dimension as 32, learning rate as 0.001, batch size as 32, and total epoch as 100;

- **Structural Features:** We use following structural features, and 32 of them are meaningful for trees:

1. number of nodes;
2. number of edges;
3. depth;
4. maximum of breadth;
5. structural virality;
6. maximum of out degree;
7. depth of the maximum of out degree node;
8. width entropy: $\sum_i p(w_i) \log(p(w_i))$, $p(w_i) = \frac{w_i}{\sum_i w_i}$, where w_i is the width of depth i ;
9. leaf node ratio;
10. average of depth;
11. variance of depth;
12. average of leaf depth;

Table C.2: Spectral bounds categorized by propagation-related structural properties.

Category	Meaning / Property	Bound Equation
C1. Branching Capacity	Max degree / Mean degree	$\bar{d} \leq \lambda_1 \leq \Delta$ [4]
	Maximum sum of degrees of adjacent nodes	$\mu_1 \leq \max_{x \sim y} (d_x + d_y)$ [4]
	Sum of top- m degrees	$1 + \sum_{i=1}^m d_i \leq \sum_{i=1}^m \mu_i$ [4]
	Mean branching	$\bar{b} \leq \frac{n\lambda_1}{2 T }$ Prop 4.1
	Maximum branching at layer k	$b_k \leq \lambda_1^2 (\lambda_1^2 - 1)^{k-1}$ Prop 4.2
	Degree entropy	$H_d \leq \log(\lambda_1^2 + 1)$ Prop 4.3
C2. Cascade Scale	Number of edges	$\frac{2e}{n} \leq \lambda_1 \leq \sqrt{2e}$ [4] $\lambda_1(\lambda_1 + 1) \leq 2e$ [4] $\sum_{i=1}^t \mu_i \leq e + \binom{t+1}{2}$ [4]
	Edge / node relation	$\lambda_1 \leq \sqrt{2e - n + 1}$ [4]
	Number of nodes	$\mu_2 \leq \lfloor \frac{n}{2} \rfloor$ [42] $\mu_1 \leq n$ [42] $\sum_i \nu_i \leq n$ [6] $\nu_{n-1} \leq \frac{n}{n-1}$ [6] $\nu_1 \geq \frac{n}{n-1}$ [6]
C3. Structural Cohesion	Separation	$\frac{ X Y }{(n- X)(n- Y)} \leq \left(\frac{\mu_1 - \mu_{n-1}}{\mu_1 + \mu_{n-1}} \right)^2$ [4] $\frac{ X Y }{n(n- X - Y)} \leq \frac{(\mu_1 - \mu_{n-1})^2}{4\mu_1\mu_{n-1}}$ [4]
	Vertex connectivity	$\kappa(G) \geq \mu_{n-1}$ [4]
	Cheeger constant	$\frac{\nu_{n-1}}{2} \leq h(G) \leq \sqrt{2\nu_{n-1}}$ [6] $h'(H) \geq \frac{\mu_{n-1}}{2}$ [25]
	Independent number	$\alpha(G) \leq \frac{-n\lambda_n}{\lambda_1 - \lambda_n}$ [4] $\alpha(G) \leq \min(\{\lambda_i \geq 0\}, \{\lambda_i \leq 0\})$ [25]
	Chromatic number	$1 - \frac{\lambda_1}{n\lambda_n} \leq \chi(G) \leq 1 + \lambda_1$ [4]
	Clique number	$\frac{n\lambda_n}{n - \lambda_1} \leq \omega(G) \leq 1 + \lambda_1$ [25]
C4. Propagation Span	Bandwidth	$b = \left\lceil \frac{n\mu_{n-1}}{\mu_1} \right\rceil$ [4]
	Structural virality	$\frac{2}{n-1} \sum_{i=1}^{n-1} \frac{1}{\mu_i}$ [32]
	Diameter	$\frac{4}{n\mu_{n-1}} \leq D(G) \leq 2\sqrt{\frac{2\Delta}{\mu_{n-1}}} \log_2 n$ [1]
	(for regular graph)	$D(G) \leq \frac{\log(n-1)}{\log\left(\frac{\nu_1 + \nu_{n-1}}{\nu_1 - \nu_{n-1}}\right)}$ [6] $D(G) \leq \text{distinct number of } \nu_i \text{ or } \mu_i - 1$ [6, 4] $m_T[0, 1] \geq (d+1)/3$ [12]
C5. Diffusion Dynamics	Random walk convergence	$O\left(\frac{\log n}{\nu_{n-1}}\right)$ [6]
	Routing time	$rt(G, \sigma) = O\left(\frac{\log^2 n}{\nu_{n-1}}\right)$ [6]
	Conductance	$\frac{\text{vol}(\delta X)}{\text{vol}(X)} \geq \frac{2\nu_{n-1}}{\nu_1 + \nu_{n-1}}$ [6]
	(coefficient of one bound)	$\frac{2\nu_{n-1}}{\nu_1 + \nu_{n-1}} \left(2 - \frac{2\nu_{n-1}}{\nu_1 + \nu_{n-1}}\right)$ [6]
	Spectral moments	m_2, m_4 [15]

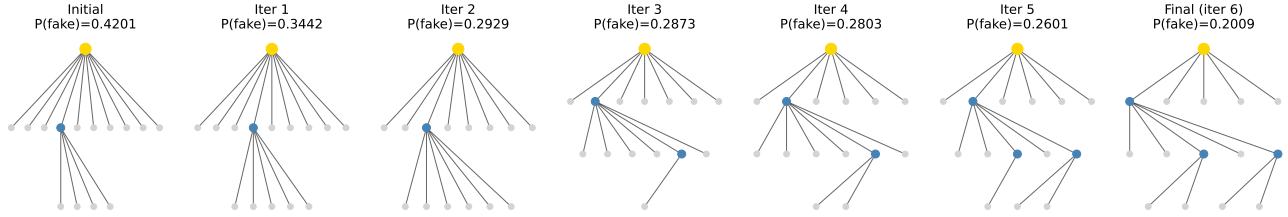


Figure C.1: Propagation graph evolution toward a more real news like structure under classifier-guided optimization. Yellow, blue, and gray nodes denote the root, internal, and leaf nodes, respectively. The title of each graph shows the current iteration t and the classifier prediction score.

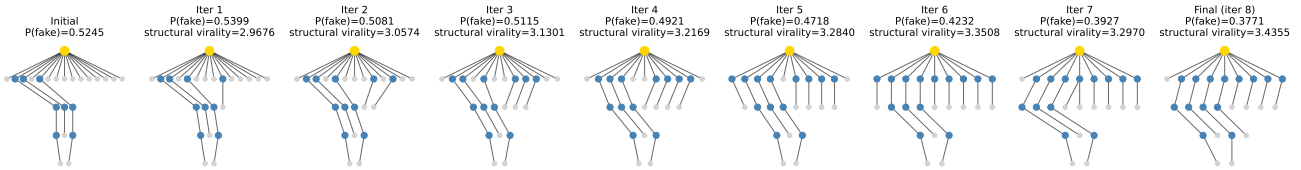


Figure C.2: Propagation graph evolution toward higher structural virality under bounds-guided optimization. Yellow, blue, and gray nodes denote the root, internal, and leaf nodes, respectively. The title of each graph shows the current iteration t , the classifier prediction score, and bound value.

13. mean branching: $\frac{\sum_{i \in I(T)} d_i}{|I(T)|}$, where $|I(T)|$ is the number of internal nodes, d_i is the degree of node i ;
14. variance of branching;
15. sackin index: $S(T) = \sum_{v \in L(T)} d(v)$, i.e., the sum of the depths of all leaf nodes, where T is a tree, $L(T)$ is a leaf node set of T , $d(v)$ is the depth of node v ;
16. colless index: $C(T) = \sum_{v \in I(T)} |L_v - R_v|$, where L_v and R_v represent number of leaf nodes in v 's left subtree and right subtree;
17. number of internal node;
18. degree entropy;
19. degree gini: $G_d = \frac{\sum_{i=1}^n \sum_{j=1}^n |d_i - d_j|}{2n \sum_{i=1}^n d_i}$, which quantifies the inequality of the degree distribution. A larger value indicates a more uneven concentration of node degrees;
20. diameter;
21. radius;
22. mean degree;
23. maximum of degree;
24. chromatic number: it is a constant number 2 for trees;
25. approximate independent number;
26. maximum of degrees of a pair of connected nodes;
27. sum of top 30% degree;
28. sum of top 60% degree;
29. $e + \binom{t+1}{2}$, where $t = 0.3 * \lfloor n \rfloor$, which is an upper bound for sum of part laplacian eigenvalues (check bounds of number of edges in Table C.2);
30. $e + \binom{t+1}{2}$, where $t = 0.6 * \lfloor n \rfloor$, which is an upper bound for sum of part laplacian eigenvalues (check bounds of number of edges in Table C.2);
31. bandwidth: $\text{bw}(L) = \max_{L_{ij} \neq 0} |i - j| + 1$, where L is the laplacian matrix of graph, which measures how far the nonzero entries of its matrix representation spread away from the main diagonal under a given node ordering;
32. wiener index: the sum of the shortest-path distances between all unordered pairs of nodes;
33. number of leaf nodes;
34. number of spanning tree: its a constant number 1 for trees;

D More Structural Optimization Results.

In addition to the two cases presented in the main text, we provide more examples of the proposed discrete structural optimization algorithms to further illustrate the differences between fake and real news dissemination patterns.

D.1 Evolution Towards More Real. We use the same initial tree as in Figure 6.1, but reverse the optimization direction to make the propagation pattern more real-like. The resulting evolution is shown in Figure C.1. By comparing it with the evolution toward a more fake-like structure, we can gain an intuitive understanding of the structural differences between fake and real news propagation.

We observe that, in Figure C.1, the tree becomes more balanced when the blue node in layer 1 is treated as the root. At the same time, its maximum breadth decreases as the structure evolves toward a more real-like pattern.

D.2 Evolution Towards Higher Structural Virality. We use the same initial tree as in Figure 6.2, but change the target bound to the structural virality bound. The resulting evolution is shown in Figure C.2. From the figure, we can see that structural virality increases monotonically. However, this result is not globally optimal, since a path graph should have a larger structural virality value. This suggests that the proposed first-order approximation method may have difficulty reaching the global optimum because it ignores higher-order terms in Eq. 5.2.

From another perspective, as structural virality increases, the tree tends to evolve toward a more real-like propagation pattern. In particular, the max-breadth decreases and the depth gap becomes smaller. These factors may be important structural cues for fake news detection.